Available online at www.sciencedirect.com
ScienceDirect
Ceramics International 37 (2011) 2287–2296
CERAMICS INTERNATIONAL
www.elsevier.com/locate/ceramint

Andalusite: An amazing refractory raw material with excellent corrosion resistance to sodium vapours

P. Prigent [a,b], M.L. Bouchetou [a,b], J. Poirier [a,b,*]

[a] CNRS-CEMHTI, 1D, avenue de la Recherche Scientifique, 45071 Orléans Cedex 2, France
[b] Ecole Polytechnique de l'Université d'Orléans, 8 rue Leonard de Vinci, 45072 Orléans Cedex 2, France

Received 15 February 2011; received in revised form 12 March 2011; accepted 14 March 2011
Available online 30 March 2011

Abstract

The chemical attack of alumina refractories by sodium vapours is far from been completely understood. In order to contribute to a better knowledge of this attack, a laboratory test was developed to simulate the sodium gaseous corrosion of different raw materials and refractories.

Corrosion of alumina raw materials by sodium vapours is due to a dissolution–precipitation process by a Na_2O rich liquid phase. The gaseous corrosion strongly depends on the microstructures and the assemblage of phases in alumina raw materials. Fire clay and andalusite raw materials exhibit very high corrosion by Na vapours. In spite of an initial high silica glass content, and as a result of trapping of the main part of the glass in the capillary network of the mullite composite crystal, mullitised andalusite leads to excellent corrosion resistance which is close to monocrystalline fused mullite.

Consequently, The use of mullitised andalusite particles in the matrix of alumina refractories limits the liquid phase formation during corrosion by sodium gas. These experimental results are in agreement with thermodynamic calculations.

Keywords: B. Electron microscopy; C. Corrosion; E. Refractories; Sodium vapours; Microstructure; Thermodynamic equilibrium

1. Introduction

At high temperature (>1000 °C) and in a reducing atmosphere, sodium vapours may cause severe corrosion of alumina refractories. Substantial improvements in resistance to gaseous corrosion were achieved for fireclay and andalusite-based refractories by reducing porosity, using well adapted raw materials and by optimizing the secondary mullite formation. However, despite advances in the development of high performance materials, corrosion mechanisms are far from being completely understood and a large number of problems remain to be solved as regards the crystallization and diffusion phenomena.

Currently, there is no selective test to evaluate the corrosion by sodium vapours of various refractory materials.

It is within this framework that a laboratory corrosion test, representative of the corrosion in industrial operating conditions, was developed in order to assess the behaviour of different raw materials and alumina refractories subjected to corrosion by sodium vapours.

The following article describes the experimental procedures used to test the materials.

Microstructures of different raw materials (fireclay, andalusite, mullitised andalusite, and fused mullite) before and after corrosion are examined to study the mechanisms of corrosion on the macro/microscale. In order to clarify the role of andalusite, several recipes of alumina refractory materials composed of andalusite and fireclay as fines particles in the matrix and/or aggregates were also submitted to the corrosion tests.

Thermodynamic predictions are compared to experimental results and the role of the liquid phase generated by sodium vapours is discussed.

2. Development of an experimental set up

A corrosion device, representative of the thermo-chemical degradations in industrial conditions, has been developed to simulate corrosion by sodium at the laboratory scale. The objectives are to compare the behaviour of alumina silicate raw materials and to select different refractory materials. Fig. 1

---

[*] Corresponding author at: CNRS-CEMHTI, 1D, avenue de la Recherche Scientifique, 45071 Orléans Cedex 2, France. Tel.: +33 2 38 25 55 14; fax: +33 2 38 63 81 03.
E-mail address: Jacques.poirier@univ-orleans.fr (J. Poirier).

0272-8842/$36.00 © 2011 Elsevier Ltd and Techna Group S.r.l. All rights reserved.
doi:10.1016/j.ceramint.2011.03.024

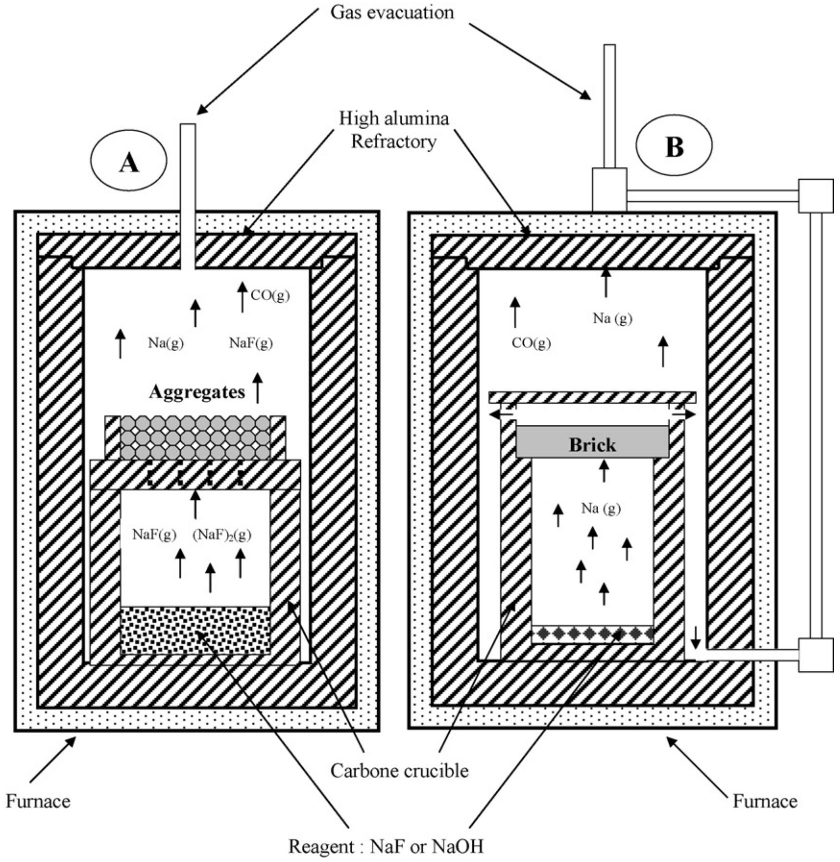

Fig. 1. Laboratory corrosion tests (A, corrosion of grains of raw materials; B, corrosion of bricks).

shows the two corrosion tests used: one is adapted for aggregates and the second for refractory materials.

The experiments take place in a reducing atmosphere. In practice, a carbon crucible is used, in order to trigger the formation of carbon monoxide at high temperature (Fig. 2). This carbon crucible is placed in a high alumina dense refractory crucible to protect the carbon from oxidation by air in the electric furnace.

All corrosion tests are done at 1300 °C (the test is at a slightly higher temperature than the real conditions in order to accelerate the reaction kinetics). This temperature is kept constant. Sodium hydroxide (NaOH) or alkali fluorine (NaF) is used as a source of gaseous sodium.

The corroded samples are studied after cooling at ambient temperature.

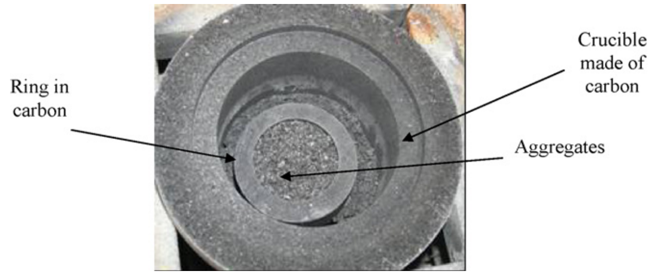

Fig. 2. Detail of the corrosion apparatus: view of grains in the carbon crucible.

The reactions, which took place during this corrosion test, are similar to those obtained in industrial conditions. Indeed, at high temperature, sodium hydroxide (NaOH) and sodium fluorine (NaF) generate gaseous Na (g) in a CO (g) environment.

The main reactions produced in this test are presented below:

$$C + O_2 \Rightarrow CO_2 \quad (1)$$

$$CO_2 + C \Rightarrow 2CO \quad (2)$$

$$2CO \Rightarrow CO_2 + C \quad (3)$$

$$2Na_{(g)} + CO \Rightarrow Na_2O_{(s)} + C \quad (4)$$

$$4NaF_{(g)} + SiO_2 \Rightarrow SiF_{4(g)} + 2Na_2O_{(s)} \quad (5)$$

At temperatures above 500 °C, the oxygen present in the carbon crucible reacts with the excess carbon to form carbon dioxide. At temperatures higher than 1000 °C, carbon dioxide reacts with carbon to give carbon monoxide [1]. At high temperatures, the atmosphere is composed of CO. At temperatures less than 500 °C, carbon monoxide is decomposed into carbon dioxide and carbon which is deposed either in the crucible or in the porosity of refractory materials. Sodium hydroxide forms gaseous sodium at temperatures higher than 1000 °C. The gaseous sodium migrates into the refractory and

Table 1
Chemical analyses of different raw materials.

Aggregates	Composition in wt%								
	Al_2O_3	Fe_2O_3	Na_2O	K_2O	SiO_2	CaO	MgO	TiO_2	Total
Fireclay	42.4	1.33	0.10	0.52	52.6	0.29	0.20	1.65	99.0
Andalusite and mullitised andalusite	58.4	1.14	0.08	0.40	38.7	0.09	0.15	0.26	99.2
Fused mullite	75.7	0.17	0.20	0.04	23.7	0.02	0.01	0.03	99.9

is then oxidised [2]. Sodium condensation occurs owing to a sufficient partial pressure of oxygen to allow the oxidation of alkali vapours. Fluorine reacts with the silica phase to form silicon tetrafluoride of silicon [2].

3. Experimental results

3.1. Gaseous corrosion of alumino silicate raw materials

Different alumino-silicate grains (fire clay, andalusite, mullitised andalusite and fused mullite) are subjected to alkaline vapours: 20 g of NaF, at 1300 °C for 12 h. The tested aggregates are grains with a similar size (1.18–1.4 mm). They are placed above the reagent. Because they have a critical effect on the corrosion resistance, the microstructures have been characterized before and after testing. The samples were polished using standard ceramographic techniques and investigated in backscattered electron (BSE) imaging mode in a JEOL JSM 6400 scanning electron microscope (SEM) equipped with an EDS spectrometer (Kevex Quantum Delta). The crystalline phases are identified by X-ray diffraction analysis (Model PW 1049/10, Philips).

Tables 1 and 2 give the chemical and mineral compositions of these raw materials. Their microstructures, before corrosion, are presented in Fig. 3.

- The fire clay aggregates are composed of mullite ($3Al_2O_3$–$2SiO_2$), cristobalite and a glassy phase. Backscattered imaging shows a heterogeneous microstructure of fine mullite crystals and a glassy phase rich in silica. A residual porosity is still present inside the grains, thus facilitating their penetration by the aggressive vapours at test temperature.
- Andalusite is a natural mineral composed of a Al_2O_3–SiO_2 single crystal or fragments of a single crystal. The main mineral impurities are quartz, biotite, ilmenite, pyrite [3]. SEM micrographic observations show that andalusite grains exhibit an initial network of cracks.
- The backscattered electron micrograph of the mullitised andalusite grain shows a mullite–glass composite [4]. When heated above 1300 °C, andalusite single crystal grains are converted into a composite of 3:2 mullite crystal with a capillary network filled with glass.
- Complete transformation: $3Al_2SiO_5 \rightarrow 3Al_2O_3–2SiO_2 + SiO_2$ leads to an 80% mullite and 20% silica rich glass [5]. Mullite crystal is topotactically oriented in relation with andalusite crystal with its *c* axis parallel to the *c* axis of the initial crystal [6]. The capillaries of glass, with diameters in the micrometer range, form interconnected tubes parallel to the *c* axis common to the mullite crystals and the parent andalusite grains.
- The microstructure of mullite is composed of a very dense fused mullite phase and a limited amount of glass. No porosity is visible.

Table 2
Mineralogical analyses of different raw materials.

Aggregates	Main phases		
Fireclay	Mullite	Glass	Cristobalite
Andalusite	Andalusite	–	
Mullitised andalusite	Mullite	Glass	
Fused mullite	Mullite	Glass	

Fig. 4 presents the microstructures of the raw materials after corrosion. SEM observations of post-mortem microstructures reveal the development of corundum crystals in a vitreous phase.

The alteration of the refractory microstructure is due to dissolution–precipitation processes by a sodium rich liquid phase (slag). The liquid phase attacks the surface of the grains, penetrates through the porosity and reacts with the initial glassy phases to yield a local liquid enriched in Na_2O that can react with the crystallize phases to form corundum. Dissolution of mullite or andalusite is greater because of the presence of secondary oxides in raw materials which provide a high amount of melt. The process is influenced by the solubility of mullite or andalusite in the slag and the initial microstructures of the raw materials [7].

SEM observations show that the fire clay and andalusite raw materials are deeply corroded by Na vapours, while mullitised andalusite and fused mullite aggregates exhibit limited attacks.

- In the case of fire clay aggregates, very fine corundum needles are embedded in a homogeneous matrix formed of glass. The morphology of these crystals shows evidence of rapid crystallization.
- For andalusite, we observe well-developed corundum needles randomly oriented in the glassy phase.
- mullitised andalusite shows a microstructure similar to that observed in the original grain, although it is partially permeated by the corrosive slag which invades the grain by capillary action and mixes with the pre-existing intergranular glass. As a consequence, mullite dissolves on the surface of the grain with a gradual increase in the amount of glass and the precipitation of corundum needles. An obvious orientation relation exists between the corundum crystals and the initial glass network of mullitised andalusite.

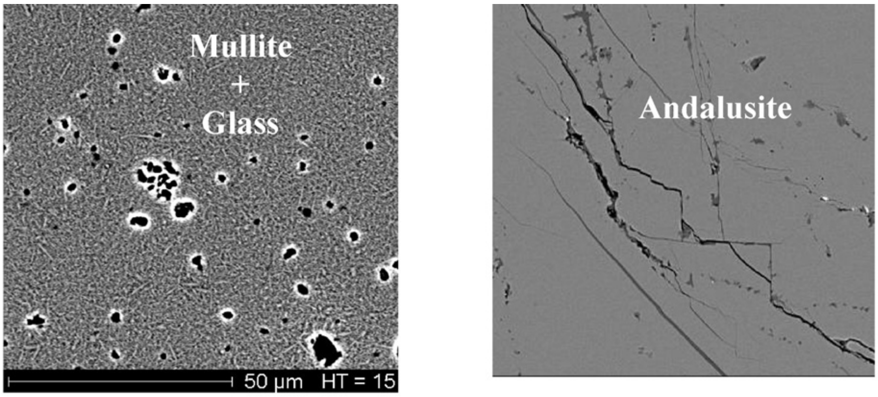

(a) clay fire aggregate

(b) andalusite aggregate

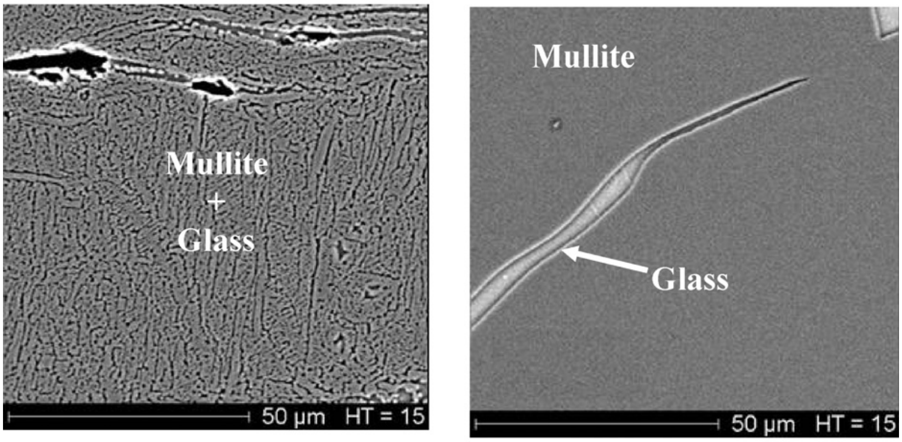

(c) mullitised andalusite aggregate

(d) fused mullite aggregate

Fig. 3. (a–d) Microstructures of aggregates of different raw materials.

- For the fused mullite, two mineral phases coexist at the corrosion interface: mullite and neoformed corundum. The chemical exchanges occur through the liquid phase. Depending on its local composition, the liquid dissolves the fused mullite which is not in equilibrium with it, and precipitates corundum phases in a preferential direction after it becomes saturated.

However, these microscopic observations are not easy to interpret. Discriminating between corundum formed during corrosion and that formed during cooling proves difficult. Two phenomena make it difficult to determine it:

- The partial crystallization of the liquid during cooling does not make it possible to assimilate the composition of residual glass (which can be determined by EDS analysis) with that of the liquid which existed at high temperature. The only representative analysis would be an EDS mapping of a zone including residual glass and the crystals formed during cooling.
- Because of the existence of newly formed solid phases in the liquid, the analyses by mapping integrate not only the crystals formed during cooling and residual glass, but also the crystals newly formed.

One possibility consists in using the analyses (obtained by EDS mapping) which are carried out on the whole of the corroded zone. The results are interpreted using the phase diagrams and the concept of ''local equilibrium'' [8].

For each raw material, Table 3 gives the composition of the vitreous phase and the composition representative of a corroded zone including residual glass and the alumina crystals (obtained by EDS mapping).

The use of the Al_2O_3–SiO_2–Na_2O ternary phase diagram and the local equilibrium rules make it possible to determine the nature of the phases at 1300 °C. The surface analysed by mapping with the scanning electron microscope (SEM) consists of the liquid and the newly formed solids during corrosion at 1300 °C. Those can be distinguished from the phases formed by the crystallization of glass during cooling.

Each composition, representative of a corroded zone including the vitreous phase and the crystals (obtained by mapping) is set on the ternary system Al_2O_3–SiO_2–Na_2O at 1300 °C (Fig. 5). For all the raw materials, except fireclay,

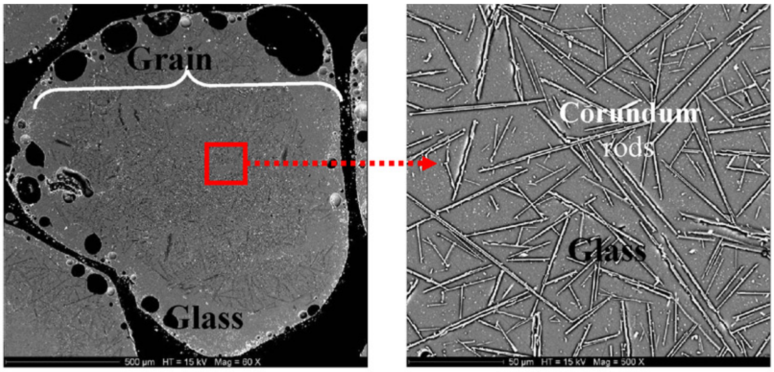

(a) clay fire aggregate

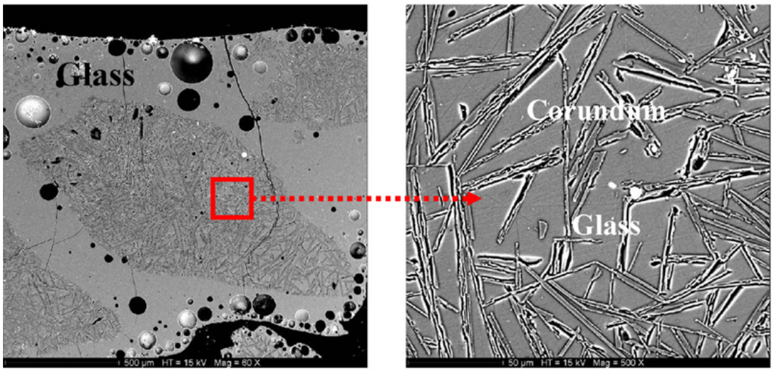

(b) andalusite aggregate

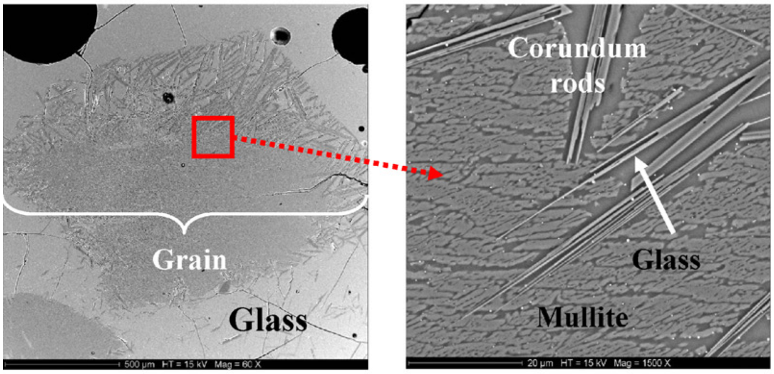

(c) mullitised andalusite aggregate

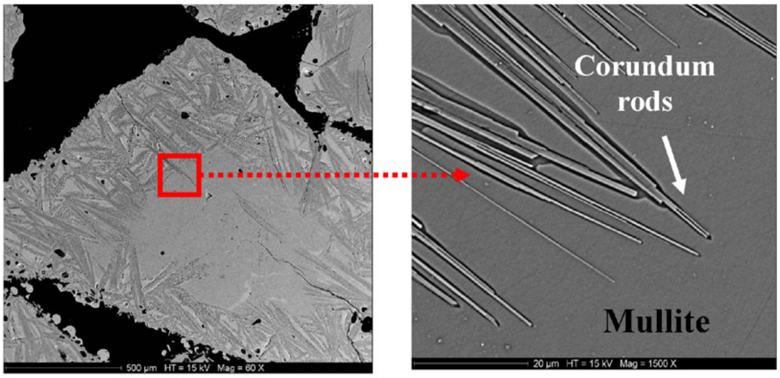

(d) fused mullite aggregate

Fig. 4. (a–d) Microstructures of aggregates of different raw materials after corrosion

Table 3
Chemical analyses of corroded aggregates (by EDS).

Aggregates (1.18–1.4 mm)	Composition of the vitreous phase			Global composition of a corroded zone including the vitreous phase and the crystals (obtained by mapping)		
	Na_2O (wt%)	Al_2O_3 (wt%)	SiO_2 (wt%)	Na_2O (wt%)	Al_2O_3 (wt%)	SiO_2 (wt%)
Fireclay	11.5	28.0	60.5	11.4	36.3	51.3
Andalusite	11.4	31.8	56.8	9.8	55.4	34.8
Mullitised andalusite	11.4	32.2	56.4	10.5	51.3	38.2
Sintered mullite	11.1	30.7	58.2	8.9	59.8	31.4

corundum is precipitated from a liquid phase at 1300 °C. Table 4 summarizes the phases formed at high temperature and after cooling.

Some important conclusions can now be drawn.

- Fire clay and andalusite raw materials exhibit very high corrosion by Na vapours. The post mortem analysis of fire clay microstructures reveals the total dissolution of mullite into the slag at the test temperature. The alumina content in the liquid phase is not enough to precipitate corundum at high temperature and the corundum needles crystallize during cooling.
- For andalusite, corundum needles precipitate in the glassy phase at 1300 °C without a significant effect to limit the corrosion.
- The gaseous corrosion strongly depends on the microstructures and the assemblage of phases in alumina raw materials. In spite of an initial high silica glass content, and as a result of trapping of the main part of the glass in the capillary network of the mullite composite crystal, mullitised andalusite leads to excellent corrosion resistance which is close to monocrystalline fused mullite.

3.2. Gaseous corrosion of alumino silicate refractories

In order to study the behaviour of fireclay and andalusite as fines particles in the matrix or/and as aggregates in alumina refractories, prototype formulations, which are well adapted to the needs of this work, have been designed. Thus, four formulations, with a low porosity, were specially formulated, according to the modified Andreasen model, to make bricks. Tables 5 and 6 give the formulation and the chemical composition of these prototype bricks. After mixing the different raw materials, bricks were pressed and fired at a temperature between 1500 °C and 1550 °C, 8 h. Some tests for characterization have been made on the new recipes. Table 7 summarizes the properties obtained.

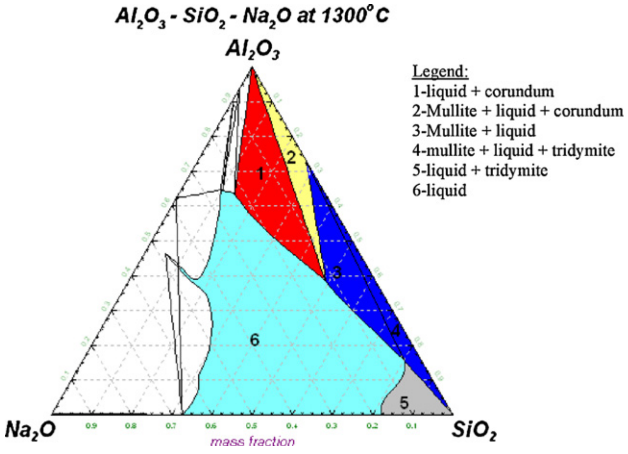

Fig. 5. System Al_2O_3–SiO_2–Na_2O at 1300 °C.

The apparent porosity is lower in bricks containing andalusite in the matrix or as aggregates: this lower apparent porosity may reduce gas penetration into the refractories. The temperatures of refractoriness under load test (R.U.L.) are higher in bricks with andalusite: the addition of andalusite in the recipes improves their hot mechanical properties.

The refractory samples were machined to obtain calibrated cylinders with a thickness of 20 mm and a diameter equal to 50 mm and were submitted to gaseous corrosion by Na (g). The corrosion tests have been done at 1300 °C. This temperature was kept constant for 5 h. A quantity of 5 g of sodium hydroxide was used as a source of gaseous sodium. This quantity was fixed in order to reach the sodium oxide content measured in corroded bricks from industrial furnaces [2,9].

Table 8 gives the amounts of mineralogical and glassy phases determined by X-ray quantitative analysis, using the ‘‘Rietveld method’’ in both the uncorroded and corroded bricks.

After corrosion, we notice:

- The glassy phase amount is higher (49 wt%) in the R1 recipe containing fireclay as aggregates and in the matrix than in the R4 formula made with andalusite grains (30 wt%).
- A significant decrease in cristobalite is observed with recipes containing fireclay: this silica phase reacts with sodium and forms a glassy phase during cooling.
- The mullite amount is lower in R1 bricks (36 wt%) than in R4 bricks (54 wt%).

Table 4
Solid and liquid phases observed at high temperature and after cooling.

Aggregates	Corrosion by Na	
	Phases observed at high temperature (1300 °C)	Phases observed after cooling
Chamotte	Liquid (100 wt%)	Corundum and glass
Andalusite	Corundum, liquid	Corundum, glass
Mullitised andalusite	Corundum, mullite, liquid	Corundum, mullite, glass
Fused mullite	Corundum, mullite, liquid	Corundum, mullite, glass

Table 5
Formulation of the alumina bricks tested.

Raw material	wt%			
	R1	R2	R3	R4
Andalusite				
1–3 mm			34	34
0–1 mm			24	24
160 μm		18		24
Fireclay				
2–4 mm	34	40		
0.2–2 mm	10	24		
0–200 μm	22		8	
0–100 μm	16		16	
Fine alumina	4	4	4	4
Clay (binder)	14	14	14	14
Alumina content (%)	46.3	49.8	55.5	58.8

Table 7
Physical properties of refractories.

	R1	R2	R3	R4
Bulk density (kg/m^3)	2256	2415	2500	2611
Apparent porosity (%)	18.6	14	15.2	13.1
Expansion coefficient (10^{-6}/°C)	5.0	5.4	5.9	7.1
Refractoriness under load				
$T_{0.5\%}$	1505	1530	1550	1560
$T_{1\%}$	1540	1560	1590	1630
$T_{2\%}$	1560	1590	1640	>1650

Table 8
Quantity phases in bricks, before and after corrosion (Reitveld method).

Recipe	Quantity (wt%)				
	Mullite	Andalusite	Cristobalite	Corundum	Glassy phase
R1 before corrosion	66	0	26	2	6
R1 after corrosion	36	0	12	3	49
R2 before corrosion	70	0	21	2	7
R2 after corrosion	50	0	7	3	40
R3 before corrosion	65	12	16	2	6
R3 after corrosion	46	12	5	4	33
R4 before corrosion	70	11	5	2	11
R4 after corrosion	54	14	0	3	30

- For R2 and R4 bricks, the quantities of glassy phases have intermediate values.
- Andalusite is detected in R3 and R4 bricks. SEM observations have shown that the andalusite aggregates, superior to 1 mm, are not totally mullitised after corrosion.

After attack by gaseous sodium, a densification of the matrices is observed due to the formation of a glassy phase (confirmed by X-ray diffraction analysis). This densification is more important in the matrices made of fireclay and clay (Fig. 6a) than in matrices made of andalusite and clay (Fig. 7a).

Corundum needles are observed in all brick matrices. The shape of corundum crystals in the case of fireclay matrices shows that it had crystallized within a liquid phase during cooling (Fig. 6b). In case of matrices made of fine andalusite particles, corundum had crystallized at a high temperature, during the corrosion test.

The mullite, resulting from the transformation of fireclay and clay at a high temperature, disappears extensively in the matrices of R1 and R3 bricks (Fig. 6b).

Fine mullitised andalusite particles are always observed in the matrix of R2 and R4 bricks (Fig. 7a). The glassy phase containing corundum needles is observed only in the initial zones corresponding to the secondary mullite made of fireclay and clay minerals and is formed outside the mullitised andalusite grains (fines particles and aggregates).

Fig. 7b shows the cartography of sodium oxide performed on R2 bricks. On this micrograph (Fig. 7a), the mullitised andalusite grains are surrounded by a white line. The cartography reveals that sodium oxide is observed in the fireclay aggregates and in the glassy phase of the matrix. There is no sodium oxide in the fine mullitised andalusite grains.

The results have shown:

- a difference of behaviour between the bricks composed of fireclay minerals and the bricks composed of andalusite minerals;
- the matrices of the bricks were more attacked than the aggregates.

Firstly, oxidation of sodium vapours preferably occurred in contact with the glassy phase resulting from the mullitisation of clay (used as a binder) and the glass expelled out of the fine andalusite grains. However, the glassy phase included in

Table 6
Chemical analyses (by XRF) of refractories.

Bricks	Composition in wt%									
	Al_2O_3	Fe_2O_3	Na_2O	K_2O	SiO_2	CaO	MgO	TiO_2	LOI	Total
R1	46.3	1.3	0.1	0.3	49.9	0.3	0.2	1.3	0.2	99.9
R2	49.8	1.2	0.1	0.3	46.9	0.3	0.1	1.1	0.1	99.9
R3	55.5	1.1	0.1	0.2	42	0.2	0.1	0.6	0.2	99.9
R4	58.8	1.0	0.1	0.2	39.1	0.2	0.1	0.4	0.1	99.8

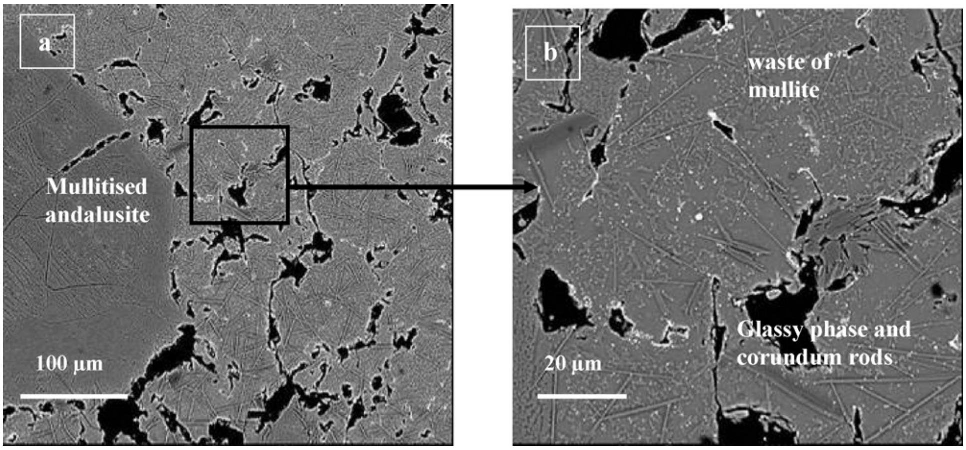

Fig. 6. Micrograph of corroded brick R3 and detail of the matrix.

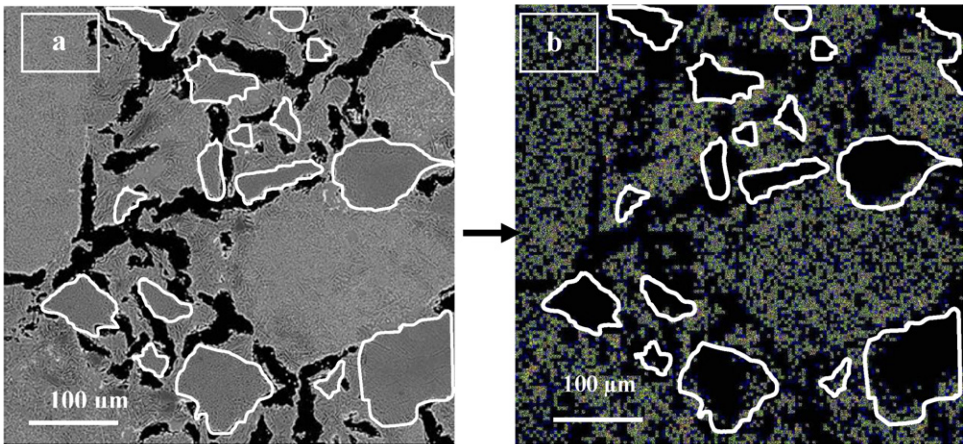

Fig. 7. Micrograph of the corroded matrix and cartography of sodium oxide of corroded matrix in brick R2 (mullitised andalusite grains are surrounded by a white line).

mullitised andalusite is not attacked by gaseous sodium corrosion. Indeed, the glassy phase is not directly accessible because it is trapped in the mullite crystal.

Secondly, to a lower degree, mullite crystals were submitted to corrosion by sodium vapours. In this case, the microstructure of crystals has an essential effect. Indeed, the mullite crystals formed from fireclay are fine acicular crystals. Nevertheless, in mullitised andalusite grains, the mullite is a monocrystal including a capillary network filled with a rich silica glass. The best corrosion resistance of the mullite formed from the andalusite mineral is due to its unique and amazing microstructure.

Thus, the use of andalusite in the matrix is advised in order to reduce the gaseous sodium corrosion of fireclay-based bricks.

4. Thermodynamic modelling

The purpose of these thermodynamic calculations is to predict the thermo chemical attack of sodium vapours on alumina refractories, to determine the phases formed at the thermodynamic equilibrium and to compare the theoretical results with micro structural observations carried out on corroded fireclay and andalusite refractories.

4.1. Description of the tools for thermodynamic calculations

Calculations are based on the minimisation of Gibb's energy of the system. It is thus possible to deduce the nature of the solid, liquid and gaseous phases, as well as their chemical composition and their reaction rate at the thermodynamic equilibrium.

Calculations have been carried out using Factsage® (version 5.4.1). Factsage is a fully integrated database and software package developed jointly between Thermfact/CRCT (Montreal) and GTT-Technologies (Aachen) [10]. It consists of a series of modules that access and manipulate thermodynamic databases and perform various calculations. Factsage® is composed of two types of thermo-chemical databases: compounds and real solutions.

- Compound databases are mainly for stoichiometric solid, liquid and gaseous species.

- Solution data are for ceramics, slag, etc. Data is stored in the form of Gibb's energy functions for the phase constituents and parameters for the excess Gibb's energy of mixing between the phases constituents. Factsage® supports several different solution models, including simple polynomial models such as the Redlich–Kister or the Legendre polynomial combined with different higher order extrapolations (Muggianu, Kohler, Toop), the quasichemical model, Pitzer parameters, and sublattice models.

The associated databases used in our study are: ELEM (elements thermodynamic database), FACT 53 (gas species, solid and liquid compounds thermodynamic database), and FT-oxid (compounds and solutions for oxides database).

The expected equilibrium phases were predicted by using the ''Equilibrium'' module of Factsage®, considering as possible phases: the slag, several solid-solution phases, and all liquid and solid compounds between the inputs.

4.2. Determination of phases at thermodynamic equilibrium

4.2.1. Liquid phase amount at high temperature

The interactions between sodium oxide (7.4 wt% of sodium vapours equivalent to 10 wt% Na_2O) and different alumina refractories, at 1300 °C, show that the higher the alumina content in the refractory, the lower the amount of liquid phase (Fig. 8). The results are in agreement with our experimental results and the observations of Silijan [11] which show that the high alumina refractory materials have a better corrosion resistance to gaseous sodium attacks.

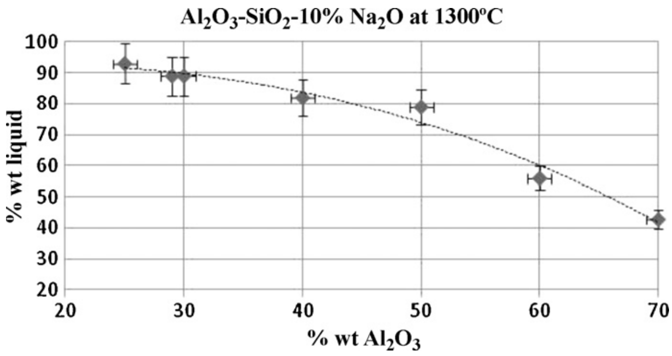

Fig. 8. Liquid phase amount (wt%) in Al_2O_3–SiO_2–10 wt% Na_2O system at 1300 °C.

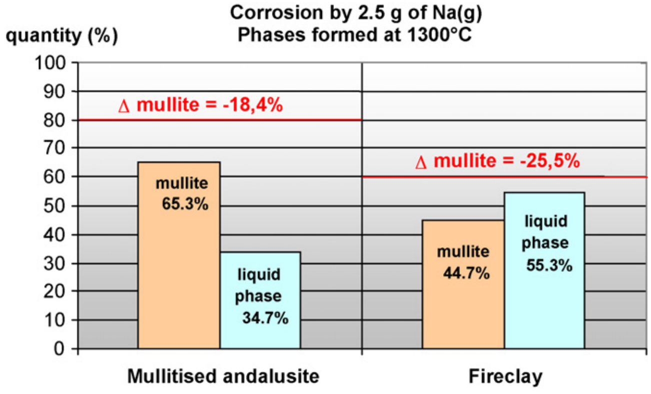

Fig. 9. Phases formed at high temperature after corrosion by 2.5% of gaseous sodium (equivalent to 3.4% of Na_2O) (▬: initial amount of mullite in the refractory).

4.2.2. Phases formed at a high temperature

Thermodynamic calculations of corrosion by sodium gas are made in two cases: fireclay (including 60 wt% mullite) and mullitised andalusite (including 80 wt% mullite) raw materials. At a high temperature (1300 °C), for 2.5 wt% of gaseous sodium (equivalent to 3.4% of Na_2O), a value close to the values measured in the corroded samples taken from industrial furnaces, the amount of mullite decreases to the benefit of rich sodium liquid phase (Table 9). The phenomenon is more significant with a fireclay mineral than mullitised andalusite (Fig. 9). The corrosion of mullitised andalusite generates a lower quantity of liquid phase compared to the fireclay. For a higher concentration of gaseous sodium (5% of Na (g) equivalent to 6.8% of Na_2O), corundum crystals are formed, at a high temperature, in the case of mullitised andalusite (Fig. 10). These thermodynamic calculations are in agreement with the experimental results.

4.2.3. Phases formed after cooling

During cooling of mullitised andalusite raw materials with lower contents of Na (g), the liquid phase crystallized into mullite and albite ($NaAlSi_3O_8$). However, in the conditions of the corrosion laboratory test, this phase is amorphous: the remaining liquid phase is transformed into a glassy phase during cooling. For a higher concentration of gaseous sodium, mullite, corundum and nepheline crystallize from the liquid phase (Fig. 11).

In the case of a fireclay mineral, for lower concentrations of Na (g), after cooling, a part of the liquid phase crystallizes into tridymite and albite.

Table 9
Quantity (wt%) and composition (wt%) of phases formed after corrosion by 2.5% of Na(g).

Composition of mullitised andalusite after corrosion by 2.5% of Na(g)				Composition of fireclay after corrosion by 2.5% of Na (g)			
Mullite: 65.3%	Liquid phase: 34.7%			Mullite: 44.7%	Liquid phase: 55.3%		
	Composition of liquid phase				Composition of liquid phase		
	%Na_2O	%SiO_2	%Al_2O_3		%Na_2O	%SiO_2	%Al_2O_3
	9.8	63.4	26.8		6.2	75.2	18.6

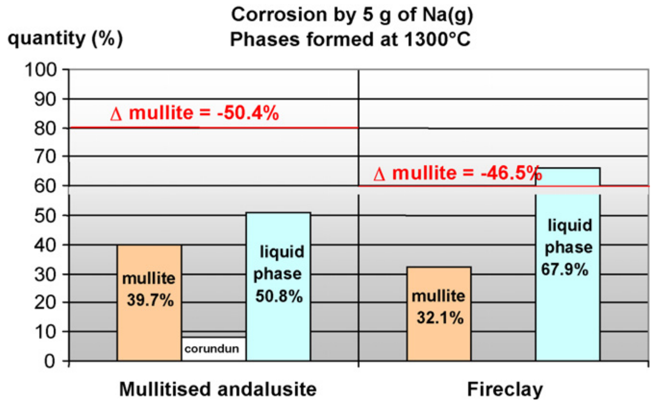

Fig. 10. Phases formed at a high temperature after corrosion by 5% of gaseous sodium (equivalent to 6.8% of Na_2O) (▬: initial amount of mullite in the refractory).

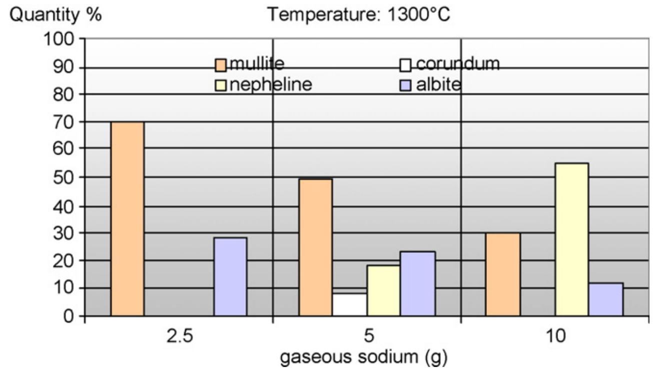

Fig. 11. Quantity of phases formed after cooling. Corrosion of mullitised andalusite by Na (g).

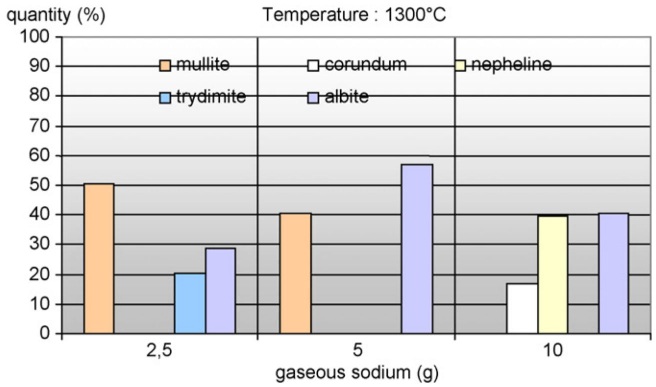

Fig. 12. Quantity of phases formed after cooling. Corrosion of fireclay by Na (g).

For higher concentration of Na (g), nepheline and corundum crystallize during cooling (Fig. 12); in experimental conditions, corundum is the only crystallized phase observed, the other phases remain glassy phases.

5. Conclusion

Corrosion of alumina refractories by sodium vapours is due to a dissolution–precipitation process by a Na rich liquid phase. The corrosion is influenced by the initial microstructures of the raw materials.

Fire clay and andalusite raw materials exhibit very high corrosion by Na vapours.

In spite of an initially high silica glass content, and as a result of trapping most of the glass in the capillary network of the mullite composite crystal, mullitised andalusite leads to excellent corrosion resistance which is close to that of monocrystalline fused mullite. For sodium concentrations close to industrial conditions, the corrosion of alumina bricks at a high temperature is located in the matrix and leads to an increase in sodium rich liquid phase. The choice of raw materials for the matrices is essential.

The use of mullitised andalusite particles in the matrix of firing refractory bricks limits the liquid phase formation during corrosion by sodium gas. In this case, the glass is trapped into a continuous network of mullite and avoids the destruction of fine mullitised andalusite grains. For fireclay raw materials, the liquid phase surrounds the acicular mullite crystals and the sodium can penetrate into the liquid phase. Thus, these matrices are more sensitive to chemical corrosion by gas sodium.

References

[1] J. Butter, A. Bongers, Alterations of anode baking furnace bricks during operation, in: J. Evans (Ed.), Proceedings of the TMS Annual Meeting Light Metals, The Minerals Metals & Materials Society, 1995, pp. 633–639.

[2] F. Brunk, Corrosion and behaviour of fireclay bricks used in the flues of open anode baking furnace, in: J. Evans (Ed.), Proceedings of the TMS Annual Meeting Light Metals, The Minerals Metals & Materials Society, 1995, pp. 641–646.

[3] M.L. Bouchetou, J.P. Ildefonse, J. Poirier, P. Daniellou, Mullite grown from fired andalusite grains: the role of impurities and of the high temperature liquid phase on the kinetics of mullitization and consequences on thermal shocks resistance, Ceramics International 31 (2005) 999–1005.

[4] W. Pannhorts, H. Schneider, The high-temperature transformation of andalusite (Al_2SiO_5) into 3/2 mullite ($3Al_2O_3$–$2SiO_2$) and vitreous silica (SiO_2), Mineralogical Magazine 42 (1978) 195–198.

[5] H. Schneider, A. Majdic, Kinetic and mechanism of the solid-state high temperature transformation of andalusite (Al_2SiO_5) into 3/2 mullite ($3Al_2O_32SiO_2$) and silica (SiO_2), Ceramics International 5 (1979) 31–36.

[6] M.L. Bouchetou, J.P. Ildefonse, J. Poirier, P. Daniellou, Production of high mullite content material from natural andalusite: influence of grain size, Refractories Applications 10 (5) (2005) 21–25.

[7] S. Zhang, H.R. Rezaie, H. Sarpoolaky, W.E. Lee, Alumina dissolution into silicate slag, Journal of American Ceramic Society 83 (4) (2000) 897–903.

[8] J.B. Thompson Jr., Local equilibrium in metasomatic processes, in: P.H. Abelson (Ed.), Researches in Geochemistry, vol. 1, John Wiley & Sons, New York, 1954.

[9] P. Prigent, M.L. Bouchetou, J. Poirier, Corrosion en phase gazeuse des réfractaires alumineux dans les fours de cuisson d'anodes destinées à la production d'aluminium, Colloque Matériaux 2006, CD-Rom, 2006.

[10] C.W. Bale, P.P. Chartrand, S.A. Degterov, G. Eriksson, K. Hack, R. Ben Mahfoud, J. Melançon, A.D. Pelton, S. Petersen, Factsage thermochemical software and databases, CALPHAD 26 (2) (2002) 189–228.

[11] O.J. Silijan, Influence of sodium on refractory behaviour in aluminium production, in: C. Allaire, M. Rigaud (Eds.), Advances in Refractories for the Metallurgical Industries IV, 2004, 115–132.